An Adaptive Backstepping Based Virtual Inertial Control Framework for DC Microgrids

Sahoo, Subham; Blaabjerg, Frede; Dragicevic, Tomislav

Published in:
2020 IEEE 11th International Symposium on Power Electronics for Distributed Generation Systems (PEDG)

DOI (link to publication from Publisher):
10.1109/PEDG48541.2020.9244327

Publication date:
2020

Document Version
Publisher's PDF, also known as Version of record

An Adaptive Backstepping Based Virtual Inertial Control Framework for DC Microgrids

Subham Sahoo*, Frede Blaabjerg* and Tomislav Dragicevic§
*Department of Energy Technology, Aalborg University, Denmark
§Department of Electrical Engineering, Technical University of Denmark, Denmark
*e-mail: sssa@et.aau.dk

***Abstract*—An adaptive backstepping based virtual inertial controller is encompassed to emulate the inertial characteristics of a synchronous machine in AC grid for a DC microgrid with various sources. This paper focuses on associating both AC and DC dynamics by estimating the angular momentum inertia and damping coefficient of the grid with the help of a voltage droop control used in the DC side. Moreover, a well-trodden power management strategy in the DC side under normal circumstances along with transition from inversion to rectification mode is proposed to increase the operational reliability. The robust performance of the proposed control strategy is tested under both simulated and experimental conditions.**

***Index Terms*—DC microgrids, virtual inertia, adaptive backstepping, grid connected systems**

I. Introduction

DC microgrids are gaining more recognition as it expedites integration of renewable energy sources with fast dynamics [1]-[2]. Bidirectional grid-connected converters (BGCs) act as the interfacing unit and are primarily responsible for controlling the energy exchange between DC microgrid and the main grid. As a secondary purpose, they are accounted for other purposes, such as DC bus voltage stability and efficiency improvement [3]. Although these sources provide fast dynamics for many grid supportive services, negligible inertia due to lack of a rotating mass facilitates instability issues in the grid.

To emulate the rotating behavior of synchronous machines with inverters, [4]-[5] have proposed virtual inertia for DC microgrids to extend grid support. The rotor inertia of the synchronous machine is emulated with the power dissipation from the energy storage in [6]. A comparative study between the dynamic characteristics between the virtual synchronous machines (VSM) and droop control is performed in [7] to conclude that VSM control adds more benefits. Additional concepts such as synchronverters [8] have also come across as a lucrative option for modular multilevel converters (MMCs) [9] and doubly fed induction generator (DFIG) based wind turbines [10] to improve the inertial support. However, the optimal power reference subject to change in AC frequency as well as oscillatory damping are significant challenges for synchronverters, which hasn't received much attention. Moreover, the authors in [11]-[12] have provided a deterministic approach to calculate the critical values and the consequent response using different values of angular momentum inertia and damping coefficient for the grid. However, the droop control used with DC voltage is not leveraged to account DC voltage dynamics and its corresponding stability bounds.

978-1-7281-6990-3/20/$31.00 ©2020 IEEE

With increased penetration from renewable energy sources, it is also important to manage the extracted energy at the same time. As DC microgrids often employ current based droop controller to stabilize DC voltage, a trade-off usually exists between the voltage deviation and power sharing accuracy [13]. Using low bandwidth communication, the reported deviation can be restored with improved power sharing accuracy [14]. Further in [15], a soft-start methodology is proposed to improve the transient characteristics during the initial start-up of power electronic converters. However, these voltage regulation methods have not yet been explored to enhance the virtual inertial response of DC microgrids. To suppress the DC voltage fluctuations in improving the inertia of DC microgrids, supercapacitors have also been widely used [16]. However, the cost of supercapacitors being very high limits this strategy in a long-term perspective as the microgrid operates in steady-state mode most of the times. As a result, it causes over-utilization of resources. In [17], a virtual inertial strategy is designed for a wind-battery based islanded microgrid by employing a high-pass filter. However, the utilization of such filters may also introduce high-frequency disturbances.

These issues have been mitigated in this paper using a non-linear control update namely, an adaptive backstepping controller to improve the inertial capabilities of DC microgrid and to estimate the inertial and damping parameters by associating the dynamics of both AC and DC counterparts. Moreover, a power management strategy between PV and battery energy storage system (BESS) is proposed to handle the intermittent behavior of renewable energy sources using a droop controller, which further assists the virtual intertial capability under the stability considerations.

The contributions of this paper are:

1) an adaptive backstepping based virtual inertial framework is proposed to estimate angular momentum inertia and damping coefficient of the grid analogous to DC voltage dynamics
2) a well-trodden power management strategy consisting of PV and BESS to assist the virtual inertial capability of the DC microgrid

The remainder of this paper is as follows. The physical topology of the grid-interfaced DC microgrid through a BGC

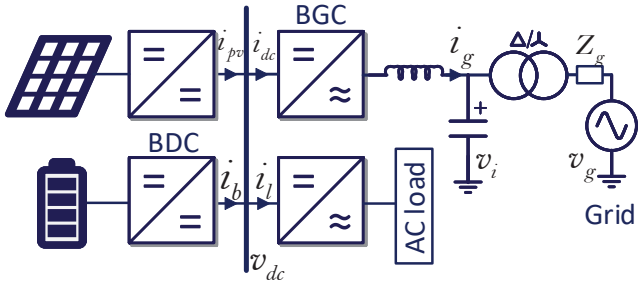

Fig. 1. Single line diagram of a DC microgrid interfaced with a three-phase bidirectional grid-connected converter (BGC).

is explained in Section II and analogized with the inertial characteristics of a synchronous machine (SM). Moreover, the motivation to use an adaptive non-linear controller will also be investigated. Section III introduces the adaptive backstepping law to estimate the inertial parameter and damping coefficients of the virtual synchronous machine. Furthermore to accommodate the virtual inertial response from the sources in the DC side, a comprehensive study of the power management strategy between the PV and BESS is carried out. Section IV provides the performance of the proposed strategy under simulated conditions with an experimental validation in Section V. Finally, Section VI concludes the paper.

II. Virtual Inertia Analogy

The system considered in this paper is shown in Fig. 1. The DC microgrid of v_{ref} = 320 V consists of a PV and battery energy storage system (BESS) connected to the DC link capacitor C_{dc} via DC/DC boost and bidirectional converters respectively. The DC microgrid is connected to the grid using a bidirectional grid-connected converter (BGC), where it is interfaced to the main grid via an input filter inductor L_i, filter capacitor C_v and a star-delta transformer. i_{pv}, i_b and v_{dc} denote the PV current, battery current and DC voltage, respectively. Furthermore, i_{dc} represent the output DC current of the full-bridge converter and i_l represent the load current.

In grid-connected mode, BGC manages the power from DC microgrid using a bidirectional energy exchange with the main grid to ensure the stability of the grid voltage. In this mode of operation, a maximum power point tracking methodology is usually employed in the DGs to extract maximum power. As a consequence, these DGs can be regarded as current sources with DC voltage regulated by the BGC.

For an AC microgrid, the basic fundamental theory of emulation of inertia, damping characteristic and primary frequency regulation is derived from the active power-frequency (P-ω) control. Assuming a single pair of pole, the mechanical equation can be written as:

$$P_{ref} - P_e - D(\omega - \omega_{nom}) = J\omega\frac{\mathrm{d}\omega}{\mathrm{d}t} \tag{1}$$

where P_{ref}, P_e, D, J, ω and ω_{nom} denote the active power reference, electromagnetic power, damping coefficient, moment of inertia, angular frequency and the rated angular frequency of the main grid, respectively. J is the moment of inertia. When the microgrid is in steady state, (1) can be rewritten as:

$$\omega = \omega_{no} - m_p P_e \tag{2}$$

where, ω_{no} is the no-load angular frequency and $m_p = 1/D_p$ is the active power droop coefficient. Translating this methodology into DC microgrids, a voltage-current (v_{dc}-i_{dc}) droop control is usually adopted. The said droop mechanism can be expressed as:

$$v_{ref} = V_{ref} - r_d i_{dc} \tag{3}$$

where, V_{ref} is the no-load DC output voltage reference of the BGC, r_d is the droop coefficient.

Similar to the ability to prevent sudden changes of frequency in AC microgrids, DC microgrids manifests virtual inertial ability to prevent sudden changes of the DC voltage v_{dc} under external disturbances. In order to maintain voltage stability of DC microgrid, BGC quickly extracts or injects i_{dc} based on the current loading condition. To formulate an analogous relationship between (2) and (3), it can be shown that ω and v_{dc}, P_e and i_{dc} are comparable in nature. The kinetic energy E_k stored in the rotor of a SM and the electrical energy E_e stored in the DC link capacitor can be given by:

$$\begin{cases} E_r = \frac{1}{2}J\omega^2 \\ E_e = \frac{1}{2}C_{dc}v_{dc}^2 \end{cases} \tag{4}$$

From this correspondence, it is obvious that many parameters are analogous between AC (containing a VSM) and a DC microgrid (containing a BGC), which has also been briefly illustrated in Table I. Extending this analogous relationship in DC microgrids, the virtual inertial dynamic equation can be represented as:

$$C_{dc}\frac{\mathrm{d}v_{dc}}{\mathrm{d}t} + D_{dc}(v_{dc} - v_{ref}) = i_{ref} - i_{dc} \tag{5}$$

where, D_{dc} and i_{ref} denote the DC damping coefficient and reference DC current, respectively.

Associating (1) and (5) for a DC microgrid, which injects/absorbs certain power based on droop coefficients for grid frequency response, (5) can be altered as:

$$J\frac{\mathrm{d}\omega}{\mathrm{d}t} - D(\omega - \omega_{nom}) = v_{dc} - v_{ref} \tag{6}$$

Since the grid parameters in (6) are usually unknown/inaccurate with limited information, an adaptive backstepping tool is proposed in this paper to provide an

TABLE I
Virtual Inertial Analogy between AC and DC Microgrid

Microgrids	AC Microgrid	DC Microgrid
Droop relationship	$P-\omega$	$v_{dc}-i_{dc}$
Control variable	ω	v_{dc}
Inertia	J	C_{dc}
Stored energy	$\frac{1}{2}J\omega^2$	$\frac{1}{2}C_{dc}v_{dc}^2$

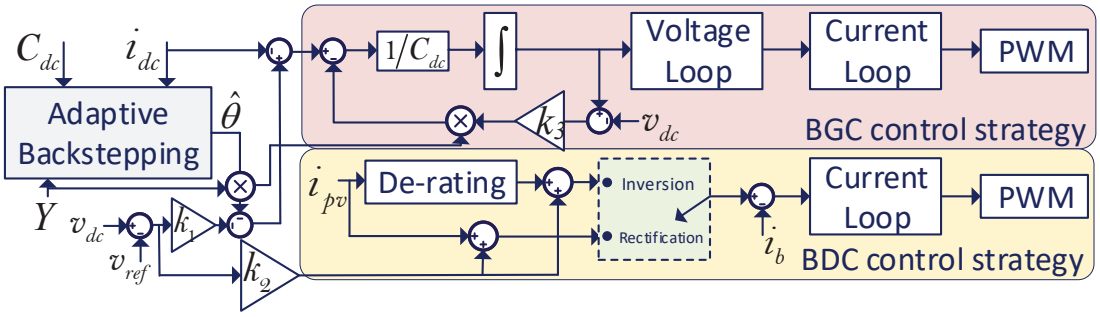

Fig. 2. Single line diagram of a DC microgrid interfaced with a three-phase bidirectional grid-connected converter (BGC) alongwith bidirectional DC/DC converter (BDC).

online update for the unknown parameters in a linearly parameterizable fashion, given by:

$$\theta = \{J \ D \ D_{dc}\} \tag{7}$$

$$Y = \{\omega_{nom} \ \omega \ v_{dc}\} \tag{8}$$

where, Y and θ denote the known/measurable and unknown parameters, respectively. Using (1)-(8), we get:

$$Y\theta + C_{dc}\frac{\mathrm{d}\eta}{\mathrm{d}t} + i_{dc} = i_{ref}. \tag{9}$$

where, $\eta = v_{dc} - v_{ref}$. It should be noted that $Y\theta$ in (9) is written to assimilate known and unknown parameters for a particular equation by parameterizing the unknown terms in a linear fashion. This serves as the motivation behind accurate estimation of the grid parameters, which require advanced non-linear control mechanisms. Hence, adaptive backstepping tool is employed in this paper to leverage accuracy in estimation of inertial parameters.

III. Adaptive Backstepping Control

The main objective is to highlight a systematic design for the development of a non-linear controller based on an adaptive backstepping approach in order to estimate the unknown parameters in θ. To synthesize a control law based on an adaptive backstepping approach, let us consider a parameter estimation error $\tilde{\theta}$, given by:

$$\tilde{\theta} = \theta - \hat{\theta} \tag{10}$$

where $\hat{\theta}$ is the estimated value. Now, let us introduce a positive definite Lyapunov candidate function:

$$V(\eta, \tilde{\theta}) = \frac{1}{2}C_{dc}\eta^2 + \frac{1}{2}\tilde{\theta}\Gamma^{-1}\tilde{\theta}^T \tag{11}$$

where Γ is a deterministic parameter, which can be varied to modify the inertial response. As (11) is positive-definite, the direct method of the Lyapunov stability is satisfied. Considering the time derivative of (11), we get:

$$\dot{V} = C_{dc}\eta\frac{\mathrm{d}\eta}{\mathrm{d}t} + \Gamma^{-1}\dot{\hat{\theta}} \tag{12}$$

since the unknown parameters in θ are not time-varying. The asymptotic stability is guaranteed only if $\dot{V}(\eta, \tilde{\theta}) < 0$. Substituting (9) in (12) to satisfy the second law of Lyapunov stability, we get:

$$\eta(i_{ref} + Y\theta - i_{dc}) \leq \Gamma^{-1}\dot{\hat{\theta}} \tag{13}$$

To achieve asymptotic stability in (13), the RHS needs to compensate for the unknown terms i_{ref} and $Y\theta$ at the same time. Hence, the power management strategy needs to accommodate coordinated generation from PV and BESS accordingly. To do so, the reference current i_{ref} from the BESS is generated based on the mode of operation of the BGC, denoted by:

$$\phi = \begin{cases} \text{Inversion}, \textbf{if } \eta > 0 \\ \text{Rectification}, \textbf{else} \end{cases} \tag{14}$$

If PV is available, it is de-rated from MPPT to a lower current generation point for providing inertial response to the grid in addition with BESS, which in turn decreases its charging current. However, in the rectification mode, BESS provides the remaining current with PV operating at MPPT. Using this principle, the reference current i_{ref} can be given by:

$$i_{ref} = \begin{cases} \rho i_{mpp} + u_{ab}, \textbf{if } \eta > 0 \\ i_{mpp} + u_{ab}, \textbf{else} \end{cases} \tag{15}$$

where i_{mpp} and ρ denote the MPPT current from PV and de-rating proportionality parameter (ranging from 0 to 1), respectively. The de-rating from PV sources is already carried out in [2]. Moreover, u_{ab} denotes the control input obtained from adaptive backstepping algorithm. The reason behind including the adaptive backstepping control input in (15) can be ascribed to charging/discharging from BESS in accordance with virtual inertial response.

Finally, we substitute θ with $\hat{\theta}$ in LHS of (13) to get:

$$\Gamma\eta(i_{ref} + Y\hat{\theta} - i_{dc}) \leq \dot{\hat{\theta}} \tag{16}$$

Replacing the estimated dynamics for θ in (16) with a tracking error trajectory to achieve asymptotic stability using:

$$r = \dot{\hat{\theta}} + K\hat{\theta} \tag{17}$$

where r denotes a tracking error. Substituting (17) into (16), we get:

$$r \geq \Gamma\eta(i_{ref} - i_{dc}) \tag{18}$$

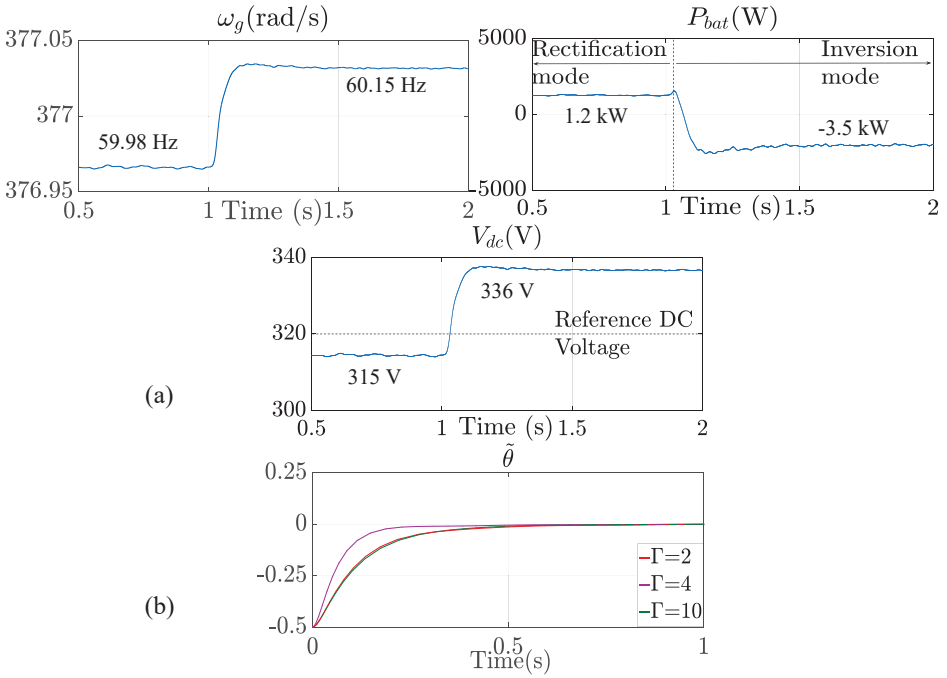

Fig. 3. Simulation results : (a) Transition from rectification to inversion mode, (b) Dynamic performance for error convergence of J for different values of the deterministic parameter Γ.

TABLE II
SYSTEM PARAMETERS OF THE BGC – SIMULATION STUDIES

Parameters	Values	Parameters	Values
v_{ref} (V)	320 V	k_{pv}	4
L (mH)	2	k_{iv}	250
$C_{dc}(\mu F)$	5650	k_{pi}	0.2
$C_v(mF)$	1.4	k_{ii}	15
k_1	7.2	k_2	10.8
k_3	9	Γ	10
ω_{no} (Hz)	60	f_{sw} (kHz)	10

with $K = \{k_1\ k_2\ k_3\}^T = -Y^T\Gamma\eta$. The design of parameters such as k_1, k_2, k_3 and Γ should be done in order to satisfy $\dot{V} \leq 0$. Using this relationship, the proposed non-linear control strategy, as shown in Fig. 2, can be used to implement virtual inertia and also accommodate power management in DC side between PV and BESS simultaneously.

IV. SIMULATION RESULTS

In order to verify the validity of the proposed control strategy, a DC-MG simulation platform is built in MATLAB/SIMULINK environment according to Fig. 1. In this system, the maximum output power of the DGs is 20 kW. The system parameters of the BGC are listed in Table II.

Fig. 3(a) shows a scenario depicting a transition from rectification mode with frequency 59.98 Hz to inversion mode with frequency 60.15 Hz. As it can be seen from Fig. 3(a), BESS responds to the frequency response at t = 1 sec as it was withdrawing 1.2 kW, but started charging with 3.5 kW. Consequently, the DC voltage settles at a higher voltage than the reference voltage of 320 V after the transition. It can also be seen that the damping coefficient, which is linked with DC dynamics provides satisfactory response without any oscillatory behavior. Furthermore, it can also be seen in Fig. 3(b) that the parameter estimation error $\tilde{\theta}$ for J settles down quickly as Γ is increased from 2 to 10. With an increase in Γ, the system is extended further into asymptotic stable region far away from the bounds leading to enhanced dynamic performance. However, this could lead to serious stability issues when the grid impedance is large, such as for a weak grid (with SCR < 1). Under these conditions, the active power transfer capability is limited as opposed to strong grid and hence the proposed controller may maloperate.

Fig. 4 shows a comparative evaluation of the estimated parameters $\tilde{J}$ and $\tilde{D}_{dc}$ with respect to different values of k_1 and k_3, respectively. It is worth notifying that the design parameters k_1 and k_3 are considered to study the response of $\tilde{J}$ and $\tilde{D}_{dc}$ in accordance with their addition to the corresponding control inputs. It can be inferred from Fig. 4 that with increase in the value of k_1 and k_3, the convergence properties of $\tilde{J}$ and $\tilde{D}_{dc}$ is improved. However, it is worth mentioning that the convergence characteristics of the adaptive control inputs need to be inline with the bandwidth of the control loop to which they are added for ensuring system stability.

V. EXPERIMENTAL RESULTS

Further, the proposed strategy has been validated on an experimental prototype (as shown in Fig. 5) of 5 kVA, 50

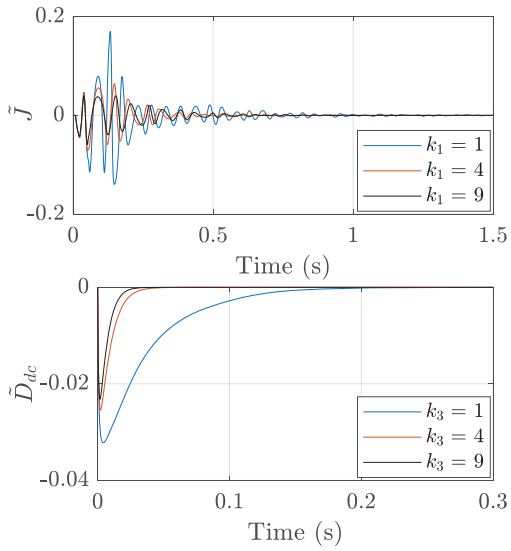

Fig. 4. Comparative evaluation of the estimated parameters $\tilde{J}$ and $\tilde{D}_{dc}$ for different values of k_1 and k_3 respectively.

TABLE III
SYSTEM PARAMETERS OF THE BGC – EXPERIMENTAL STUDIES

Parameters	Values	Parameters	Values
v_{ref} (V)	320 V	k_{pv}	0.6
L (mH)	3	k_{iv}	32
$C_{dc}(\mu F)$	3400	k_{pi}	0.75
$C_v(mF)$	1.4	k_{ii}	60
k_1	0.8	k_2	2.7
k_3	3.4	Γ	4
ω_{no} (Hz)	50	f_{sw} (kHz)	10

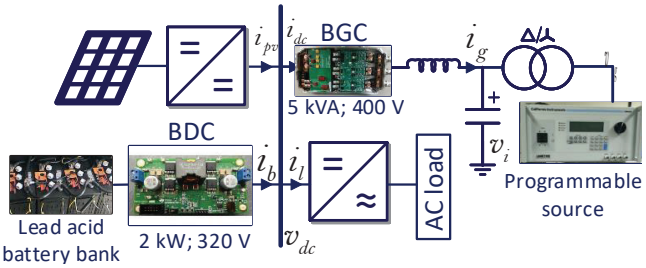

Fig. 5. Experimental prototype used to validate the proposed control strategy.

Hz BGC controlled by a National Insturments sbRIO 9606 directly connected to a 4-quadrant AMETEK CSW5550 programmable AC source. The power ratings of the associated converters are also highlighted in Fig. 5. The experimental parameters are listed in Table III.

It can be seen in Fig. 6 that the transition from rectification (49.2 Hz) to inversion (52.36 Hz) mode to rectification again (47.85 Hz) is carried out swiftly in the presence of the proposed virtual inertial control strategy, which responds to the change in grid frequency. Further, it can be seen that the said transitions are well supported by the proposed power

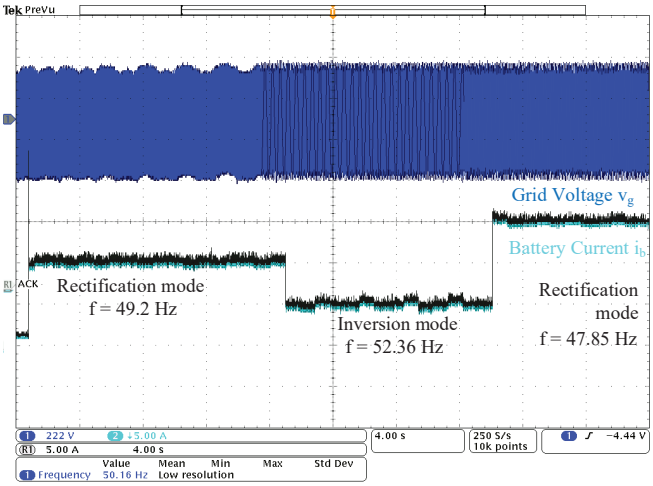

Fig. 6. Experimental result for transition from rectification (49.2 Hz) → inversion (52.36 Hz) → rectification (47.85 Hz) mode for a reference frequency of 50 Hz.

management in DC microgrid without any pre-calculated knowledge of the inertial and damping coefficients. Basically, a pre-historic knowledge of these parameters are also subjected to network reconfiguration, where many generators are continually being added to power grid, thereby continually changing these parameters.

VI. CONCLUSION

This paper proposes a virtual inertial control framework for DC microgrids by associating dynamics of both AC and DC sides using an adaptive backstepping controller. This strategy can be used as a generalized standard to estimate the grid inertia and damping coefficient for grid connected DC microgrids and enhance the virtual inertial response for a particular frequency disturbance in the grid. It provides a comprehensive way of designing the unknown inertial parameters which greatly affects the grid-supportive response of BGC. To accommodate the available energy sources and enforce maximum utilization of resources, a well-trodden power management has also been designed for PV and BESS in the DC microgrid. Its robustness under different operation modes and its response for varying values of gains have been verified under simulated and experimental conditions. To extend future scope of work, the performance of the proposed controller will be studied for a BGC directly interfaced to weak grid, where the active power transfer capability is highly affected, thereby affecting the dynamics in (1). Furthermore, the virtual inertial response from DC microgrid involving fuel cells and supercapacitors will be also be studied in the future.

REFERENCES

[1] J. J. Justo, F. Mwasilu, J. Lee, and J. W. Jung, "AC-microgrids versus DC-microgrids with distributed energy resources: A review," *Renew. Sustain. Energy Reviews*, vol. 24, pp. 387-405, 2013.

[2] S. Sahoo and S. Mishra, "A Multi-Objective Adaptive Control Framework in Autonomous DC Microgrid,", *IEEE Trans. Smart Grid*, vol. 9, no. 5, pp. 4918-4929, 2017.

[3] D. Chen, X. Lie, and L. Yao, "DC voltage variation based autonomous control of DC microgrids," *IEEE Trans. Power Delivery*, vol. 28, no. 2, pp. 637-648, 2013.
[4] M. F. M. Arani, E. F. El-Sadaany, "Implementing virtual inertia in DFIG-based wind power generation," *IEEE Trans. Power Syst.*, vol. 28, no. 2, pp. 1373–1384, 2013.
[5] S. D'Arco, and J. A. Suul, "Virtual synchronous machines—Classification of implementations and analysis of equivalence to droop controllers for microgrids," *PowerTech (POWERTECH), IEEE Grenoble*, pp. 1–7, 2013.
[6] H. P. Beck and R. Hesse, "Virtual synchronous machine," *Proc. 9th Intl. Conf. Elect. Power Quality Utilisation*, Barcelona, Spain, pp. 1-6, 2007.
[7] J. Liu, Y. Miura, and T. Ise, "Comparison of dynamic characteristics between virtual synchronous generator and droop control in inverter based distributed generator," *IEEE Trans. Power Electron.*, vol. 31, no. 5, pp. 3600–3611, May 2016.
[8] Q. C. Zhong, and G. Weiss, "Synchronverters: Inverters that mimic synchronous generators," *IEEE Trans. Ind. Electron.*, vol. 58, no. 4, pp. 1259–1267, 2011.
[9] C. Li, J. Xu, and C. Zhao, "A coherency-based equivalence method for MMC inverters using virtual synchronous generator control," *IEEE Trans. Power Del.*, vol. 31, no. 3, pp. 1369–1378, Jun. 2016.
[10] S. Wang, J. Hu, X. Yuan, and L. Sun, "On inertial dynamics of virtual synchronous-controlled DFIG-based wind turbines," *IEEE Trans. Energy Convers.*, vol. 30, no. 4, pp. 1691–1702, Dec. 2015.
[11] J. Liu, Y. Miura, H. Bevarani, and T. Ise, "Enhanced Virtual Synchronous Generator Control for Parallel Inverters in Microgrids," *IEEE Trans. Smart Grid*, vol. 8, no. 5, pp. 2268-2278, 2017.
[12] D. Chen, Y. Xu, and A. Q. Huang, "Integration of DC microgrids as virtual synchronous machines into the ac grid," *IEEE Trans. Ind. Electron.*, vol. 64, no. 9, pp. 7455-7466, 2017.
[13] J. Schonberger, R. Duke, and S. Round, "DC-bus signaling: a distributed control strategy for a hybrid renewable nanogrid," *IEEE Trans. Ind. Electron.*, vol. 53, no. 5, pp. 1453–1460, Oct. 2006.
[14] S. Sahoo and S. Mishra, "A Distributed Finite-Time Secondary Average Voltage Regulation and Current Sharing Controller for DC Microgrids," *IEEE Trans. Smart Grid*, vol. 10, no. 1, pp. 282–292, 2017.
[15] S. Shin, H. Lee, Y. Kim, J. Lee, and C. Won, "Transient response improvement at startup of a three-phase AC/DC converter for a DC distribution system in commercial facilities," *IEEE Trans. Power Electron.*, vol. 29, no. 12, pp. 6742–6753, Dec. 2014.
[16] B. Liu, F. Zhuo, and X. Bao, "Control method of the transient compensation process of a hybrid energy storage system based on battery and ultra-capacitor in micro-grid," *Proc. IEEE ISIE Conf.*, pp. 1325–1329, 2012.
[17] X. Zhu, J. Cai, Q. Yan, J. Chen, and X. Wang, "Virtual inertia control of wind-battery-based islanded DC micro-grid," *Proc. IET RPG Conf.*, pp. 1–6, 2015.